

Safe Control of Gas Engine in Transient Condition

by

Oleksiy BONDARENKO*, Yasuhisa ICHIKAWA*, Tetsugo FUKUDA*

ガスエンジン動特性の制御改善

オレクシー ボンダレンコ、市川 泰久、福田 哲吾

Abstract

In the field of marine application, natural gas fueled engine is a promising successor of Diesel engine, owing to lower emissions and fuel cost. However, the marine application imposes vast requirements on transient responses, such as the fast response to load demand during a ship maneuvering, rejection of large load fluctuation in rough weather condition, etc. Moreover, engine can be coupled to a fixed pitch propeller (FPP), controllable pitch propeller (CPP) or electric generator specifying various modes of operation. In respect that the gas engine combustion process differs from that in Diesel engine, the load acceptance is subject to specific limitation due to a knock and misfiring phenomena. Thus, for the gas engine to be efficient and safe propulsion unit, it is necessary to consider the problems related to transient response behavior and develop countermeasures.

This paper employs mean value approach for constructing the engine model where non-linear dynamics are modelled from the first principles using available non-linear characteristics of essential components. In order to capture the particularities inherent to the gas engine, notably air throttle valve and fuel gas admission valve, the nonlinear model of components has been developed and discussed in details. The nonlinear model is parametrized from the engine test data and model fitness is then confirmed. Finally, the paper discusses the derivation of a linearized model of the target engine which is necessary for transfer function model describing the transition from the inputs to the desired outputs. The transfer functions constituent parameters can be readily obtained from the fully parametrized nonlinear model at any operating point, thus facilitating study on engine control system and uncertainty of model parameters.

* 環境・動力系

原稿受付 平成27年11月16日

審査日 平成28年1月27日

Contents

1. Introduction	50
2. Experiment and Measurement System	50
2.1 Experimental setup	50
2.2 Compressor speed estimation	51
3. Mean Value Engine Model (MVEM)	52
3.1 Overview	52
3.2 Engine rotational dynamics	52
3.3 Charge air receiver	53
3.4 Exhaust gas receiver	54
3.5 Turbo-compressor rotational dynamics	55
4. Model Tuning and Validation	56
4.1 Air throttle and fuel admission valve characteristics	56
4.2 Model stationary similarity	58
4.3 Model dynamics similarity	58
5. The Model Utilization	59
5.1 Control systems study	60
5.2 Linearized state space engine model	61
5.3 Analysis of system robustness	64
6. Conclusions	65
References	66

Abbreviations

f_{cf} : compressor blade frequency [Hz]
n_{tc} : turbo-compressor speed [s^{-1}]
N_{bl} : compressor blade number [-]
n_e : engine speed [s^{-1}]
I_e : engine moment of inertia [$m/s^2 \text{ kg}$]
Q_e : engine torque [Nm]
Q_l : load torque [Nm]
Q_i : indicating torque [Nm]
Q_{fr} : torque of friction force [Nm]
Q_p : torque of pumping stroke [Nm]
z_c : number of engine cylinders [-]
V_s : swept volume of cylinder [m^3]
imep: mean indicating pressure [Pa]
p_s : scavenging air manifold pressure [Pa]
p_e : exhaust gas manifold pressure [Pa]
$m_{f.c}$: fuel mass per cycle [kg]
G_{fv} : fuel valve mass flow [kg/s]
F_{fv} : effective fuel valve area [m^2]
p_f : fuel gas pressure [Pa]
k_f : fuel gas specific heats ratio [-]
T_s : scavenging air manifold temperature [K]
T_c : compressor outlet temperature [K]
T_w : cooling water temperature [K]
G_{tv} : air mass flow through throttle valve [kg/s]
G_a : air mass flow through engine [kg/s]
$V_{a.r}$: air manifold volume [m^3]
η_v : engine volumetric efficiency [-]
R_a : air gas constant [J/(kg K)]
k_a : air gas specific heat ratio [-]

G_{tr} : air mass flow trapped in cylinder [kg/s]
 G_{scv} : scavenging air mass flow [kg/s]
 \tilde{A}_v : scavenging effective area [m^2]
 F_{tv} : projected area of the valve flap [m^2]
 p_c^* : pressure of turbo-compressor [Pa]
 μ^* : flow coefficient of throttle valve [-]
 r_p : radius of throttle valve pipe [m]
 r_v : radius of throttle valve flap [m]
 p_a : ambient air pressure [Pa]
 T_a : ambient air temperature [K]
 G_f : fuel gas mass flow [kg/s]
 $m_{e,r}$: mass of exhaust gas in manifold [kg]
 T_e : exhaust gas temperature (before turbine) [K]
 R_e : exhaust gas constant [$J/(kg K)$]
 $C_{p,e}$: specific exhaust gas heat (at constant pressure) [$J/(kg K)$]
 $C_{p,a}$: specific air gas heat (at constant pressure) [$J/(kg K)$]
 k_e : exhaust gas specific heat ratio [-]
 $V_{e,r}$: exhaust gas manifold volume [m^3]
 H_u : lower calorific value of fuel [J/kg]
 a_t : turbine flow area correction factor [-]
 \tilde{A}_t : turbine effective flow area [m^2]
 η_{ic} : compressor isentropic efficiency [-]
 η_{it} : turbine isentropic efficiency [-]

Subscript "0" denotes value of variables at nominal operating mode of the engine

1. Introduction

Gas-fueled engines (both pure gas and dual fuel) in the last decades have been recognized as a superior drive for shore-based power generating plants, largely owing to their high efficiency, lower emissions and attractive fuel price as compared to the Diesel engines. In last years, the gas-fueled engines are beginning to spread in the marine sector too, where traditionally Diesel/HFO engines are commonly used. Especially, the application of gas engines on a Platform Supply Vessels, Ferries and other coastal and inland vessels as a prime propulsion unit is highly beneficial due to the strict emission regulation applied on coastal areas. Despite the benefits provided by the gas engines there is still an uncertainty about the suitability of these engines for marine applications due to weak transient response prone to abnormal combustion occurrence.

In gas-fueled engines abnormal combustion is characterized by a sudden pressure rise in some parts of cylinder charge which is commonly referred to as knock. The likelihood of knock occurrence and its intensity depends on many operational parameters of engine such as methane number of fuel, advance angle of ignition, air charge temperature, air excess ratio, etc. In transient condition such as load acceptance, when the power of engine is adjusted by increasing the fuel gas admission time through a port valve, the amount of combustion air, for a certain period of time, remains the same due to a turbocharger delay and the engine runs temporarily with the reduced air excess ratio (rich mixture). In such a condition, the formation of knock is likely to occur and as justified in [1] the formation of knock is expected for mixtures close to stoichiometric, specifically for air excess ratio $\lambda < 2$. Moreover for modern engine design the parameters are calibrated to provide highest thermal efficiency of engine at reduced knock margin, this consequently leads to reduction in safety limits. In this respect, the control organization of gas-fueled engines is more challenging than that in Diesel engines and requires not only information about engine rotational speed but also knowledge of the air flow state. One of the solutions to this problem is to include physical models of the relevant engine subsystems in the control system and using model-based feedback control to compensate for slow dynamics of the turbocharger. Therefore the development of a proper dynamic model of engine is of great importance.

2. Experiment and Measurement System

2.1 Experimental setup

The data necessary for simulation model identification were collected on an AYG20L engine designed by Yanmar. The AYG20L is a four-stroke, high speed engine that operates on natural gas with a lean-mixture – Otto cycle. The air excess ratio at nominal operating mode is kept in the vicinity of 2. The fuel gas is supplied into intake port through admission valves installed at each cylinder. The gas is injected during the intake stroke and amount is controlled by admission time in accordance with Engine Control Unit (ECU) command. The spark ignition (SI) system of each cylinder includes pre-chamber and spark plug. Besides, the engine is equipped with a throttle valve between turbo-compressor and charge air manifold. This valve is designated to keep air excess ratio above knock limit adjusting air pressure in the intake manifold with respect to engine load. Its control system consists of a static map stored in ECU and the parameters of map are available for adjustment.

The engine is directly coupled to an alternator, which in turn can be loaded by the ballast resistors. The main specifications of the engine employed in this study are listed in the Table 1 whereas the Fig.1 shows a basic configuration of the experiment and measurement system.

The measurement system includes pressure and temperature sensors across the engine key components such as air charge receiver, exhaust gas receiver, throttle valve, etc. In addition the pressure sensors were installed on the cylinder No 6 (the opposite to the flywheel) to provide readings of in-cylinder, inlet and outlet ports pressures synchronized with the crankshaft angle with the resolution of 0.5° . The ignition timing was detected from the measured value of the spark plug current. Since the engine, used in experiment is a mass-produced engine, there are no special devices to measure air or exhaust gas flow installed on it. The exhaust gas mass flow, as well as, air mass flow necessary for estimation of air excess ratio λ were calculated on the carbon balance method based on measured exhaust gas composition. Last but not least, the small commercial engines usually doesn't include turbocharger speed sensor and experimental engine is not an exception to the rule. However the turbocharger speed is important measure of compressor performance and is necessary parameter for simulation model identification. In order to overcome this deficiency, a non-intrusive method of compressor speed estimation was developed.

Table 1. AYG20L engine specification

Engine type	[-]	Four-stroke, Lean burn, SI / Pre-chamber
Cylinders	[-]	6 (in line)
Bore x Stroke	[mm]	155 x 180
Power	[kW]	434
Rated Speed	[rpm]	1800
BMEP	[bar]	14.0
Mean piston speed	[m/s]	10.8

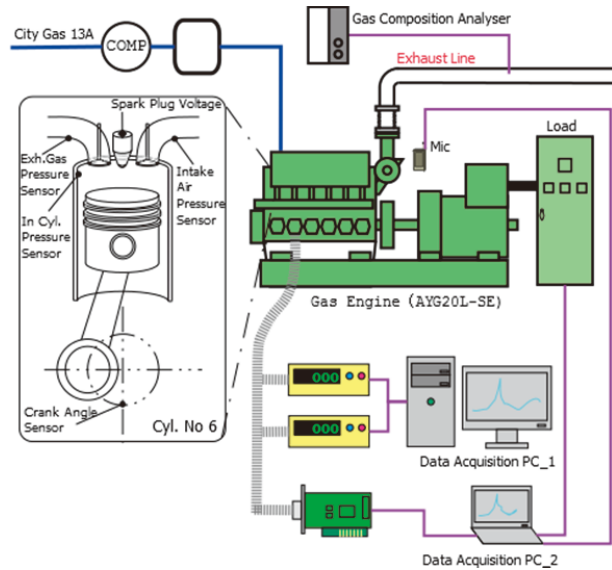


Fig.1 Measurement system configuration

2.2 Compressor speed estimation

The modern medium and high speed commercial engines, as a rule, are not equipped with the turbo-compressor speed pickup. However, the compressor is a source of vibro-acoustic field, the frequency spectrum of which includes frequency component corresponding to compressor's blade frequency, defined as follows:

$$f_{cf} = n_{tc} N_{bl} \tag{1}$$

Thus the task of speed estimation comes to a measurement of compressor acoustic emission, calculation of a power spectrum and determination of carrier frequency. Since the spectrum consists of frequency components multiple to the desired frequency, the analysis interval has to be bounded within the frequencies of compressor's operating range. Furthermore the measured acoustic emission is the combination of useful signal and noise and the secure determination of carrier frequency is a challenging task. Thus for spectral density estimation the Welch's method was employed: that is, it is a modified periodogram spectrum estimate in that, it reduces noise in the estimated power spectrum. Further, the effect of "leakage" resulting from the Fourier's transformation is effectively suppressed by application of the Kaiser-Bessel-Derived (KBD) window. Finally, the validity of proposed method was confirmed through comparison of estimated speeds with that obtained from the available compressor map, the results are shown in Fig.2.

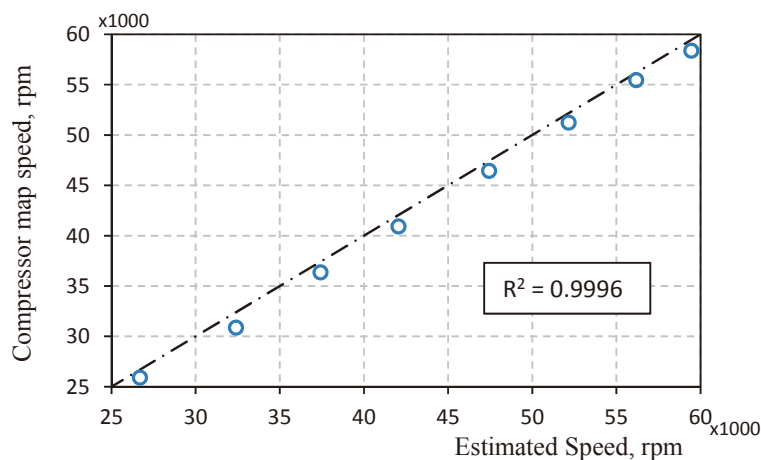


Fig.2 Compressor speed estimation based on noise emission analysis

It is worth to mention that the experience of utilization above described method confirmed its robustness and short estimation time (the speed value is updated on interval less than 100 ms), which enabled the measurement of the compressor speed in transient regime, as will be shown further. Also it set prerequisites for utilization of the developed non-intrusive method of turbo-compressor speed pickup in engine control system.

3. Mean Value Engine Model (MVEM)

3.1 Overview

Control of engines ensuring knocking free transient response is a key factor to increase efficiency and safety of propulsion engines operating on gas fuel according to the Otto cycle. However, all internal combustion engines contain significant nonlinearities which dominate their dynamic behavior, and the only way to design robust and efficient engine control system is to use the dynamic model of the engine. In recent time the so called mean value engine models (MVEM) has been successfully applied in a field of engines dynamic modeling. Thus in [2] the MVEM of SI gasoline engine has been developed, further in [3] the mean value modelling approach was applied on a propulsion system with Diesel engine, finally Hansen et al. have extended the mean value approach to Diesel engine with Exhaust Gas Recirculation (EGR) system⁴⁾.

Mean value engine models predict the values of engine thermodynamic states as well as mechanical dynamic states on the basis of the engine cycle averaging. The main advantage of the MVEM modelling approach is that the model is physically based and gives good dynamic description of engine behavior with sufficient steady-state accuracy. Owing to the philosophy of mean value approach, the simulation model of the lean-burn gas engine can be easily developed taking into account the particularities inherent to the engine. A generic MVEM for a turbocharged engine consists of four important subsystems which describe behavior of the charge air manifold, the exhaust gas manifold, the acceleration of engine shaft and the acceleration of turbo-compressor shaft. Besides, the particular attention has to be drawn to the important parts of the model such as: the manifold pressure state with further attention to the throttle valve and the gas fuel admission valve. This is because the charge air pressure determines instantaneous air mass flow to the engine including effect of the filling or emptying of the intake manifold with air during throttle opening and closing. In turn, the fuel gas admission valve controls engine power adjusting fuel gas flow to the engine. Thus the combined action of these two subsystems determines air/fuel ratio which primarily affects the knock intensity. The detailed description of engine model constituent sub-models is discussed in the subsequent chapters.

3.2 Engine rotational dynamics

In the case of propulsion system, the shaft speed responses to changes in load or to changes in speed ordered by the governor are of prime interest. Thus, the simulation model construction starts from the state equation of engine shaft speed n_e which is based on the Newton's second law and yields equation of torques balance:

$$2\pi I_e \frac{dn_e}{dt} = Q_e(n_e, p_s, \dots, t) - Q_l(t) \quad (2)$$

The solution of this equation depends upon the explicit definition of constituent torque functions, that is the engine torque Q_e and load torque Q_l . The load torque can either be provided by a propeller or alternator and for a detailed discussion on these models see [5], [6]. The engine torque is composed of indicated torque Q_i , friction losses torque Q_{fr} and torque of pumping losses Q_p :

$$Q_e = Q_i - Q_{fr} - Q_p \quad (3)$$

For the calculation of cylinder friction, the typical approach consists of the use of empirical correlation with the relative engine speed change and relative change of indicated mean effective pressure (imep):

$$Q_{fr} = \frac{0.5z_c V_s}{2\pi} \left(k_{fr0} + k_{fr1} \frac{\text{imep}}{\text{imep}_0} + k_{fr2} \frac{n_e}{n_{e0}} \right) \quad (4)$$

Torque of pumping stroke losses is considered proportional to charge air and exhaust gas pressures difference:

$$Q_p = \frac{0.5z_c V_s}{2\pi} (p_s - p_{exh}) \quad (5)$$

The last remaining term in Eq.3, notably the engine indicating output Q_i , can be found proportional to the fuel quantity $m_{f,c}$ supplied per cycle:

$$Q_i = K_{p_i} m_{f,c} \eta_c, \quad \therefore K_{p_i} = \frac{0.5z_c V_s \text{ imep}_0}{2\pi m_{f,c_0}} \quad (6)$$

Here it should be noted that a correction coefficient η_c (also referred to as relative thermal efficiency) is introduced in Eq.6 to account for non-linearity between imep and admitted fuel quantity, as can be found in [7].

At this point, the discussion on MVEM has arrived to the first noteworthy difference of the developed model of gas engine from that of Diesel engine, notably calculation amount of gas fuel supplied per cycle or in other words mathematical model of gas admission valve. Assumptions that the valve opening and closing time is infinitesimal and pressure settle time is negligible, allow to characterize the mass flow through the valve by a nozzle orifice equation:

$$G_{fv} = F_{fv} \frac{p_f}{\sqrt{R_f T_f}} \sqrt{2 \frac{k_f}{k_f + 1} \left[\left(\frac{p_s}{p_f} \right)^{\frac{2}{k_f}} - \left(\frac{p_s}{p_f} \right)^{\frac{k_f+1}{k_f}} \right]}, \quad \therefore F_{fv} = f \left(\frac{p_f}{p_s} \right) \quad (7)$$

Here the effective valve area F_{fv} is the empirical polynomial function of pressure ratio across the valve.

Thus the mass of gas supplied per cycle is determined by the ECU which controls the gas admission time d_{inj} :

$$m_{f,c} = G_{fv} d_{inj} \quad (8)$$

3.3 Charge air receiver

The engine charge air receiver is considered as a control volume which receives the air from the compressor through the throttle valve; on the other hand the engine consumes air from the receiver. The resulting air masses balance determines the rate of pressure change in the manifold and can be described by the ideal gas state equation:

$$\frac{dp_s}{dt} = \frac{R_a T_s}{V_{a,r}} (G_{tr} - G_a) \quad (9)$$

It is assumed that the temperature of air T_s in the receiver is constant and is governed by an intercooler as follows:

$$T_s = T_c - (1 - d_{ic} G_a) (T_c - T_w) \quad (10)$$

In the case of four stroke cycle engine, the total mass of air G_a passed through the engine is composed of air trapped in a cylinder during pump stroke and air passed through during inlet/exhaust valves overlap. In turn the trapped air mass flow G_{tr} is determined by the engine swept volume V_s , engine speed and volumetric efficiency η_v :

$$G_{tr} = \frac{0.5 z_c V_s p_s n_e \eta_v}{T_s R_a}, \quad \therefore \eta_v = f(n_e^2) \quad (11)$$

The scavenging air mass flow G_{scv} through the engine can be considered similar to that through a restriction with area equal to mean effective area \tilde{A}_v of valves overlap time-cross section:

$$G_{scv} = \tilde{A}_v \frac{p_s}{\sqrt{R_a T_s}} \sqrt{2 \frac{k_a}{k_a + 1} \left[\left(\frac{p_e}{p_s} \right)^{\frac{2}{k_a}} - \left(\frac{p_e}{p_s} \right)^{\frac{k_a+1}{k_a}} \right]} \quad (12)$$

$$G_a = G_{tr} + G_{scv} \quad (13)$$

Last, but not least algebraic equation to complete description of the charge air manifold dynamics is that which is used to describe the air mass flow G_{tv} past the throttle valve. This valve imposes high pressure loss and operates at high flow velocity, thus the model for compressible flow through a nozzle orifice has to be used:

$$G_{tv} = \mu^* F_{tv}(\alpha) \frac{p_c^*}{\sqrt{R_a T_c}} \sqrt{2 \frac{k_a}{k_a + 1} \left[\left(\frac{p_s}{p_c^*} \right)^{\frac{2}{k_a}} - \left(\frac{p_s}{p_c^*} \right)^{\frac{k_a + 1}{k_a}} \right]} \quad (14)$$

The mass flow through the air supply system “compressor-throttle-manifold” is affected by the valve flap set angle α , controlled by ECU and pressure output p_c^* of the turbo-compressor. The effective flow area of the valve is composed of two variable parameters:

- the projected area of the valve flap at the center plane of the pipe F_{tv}

$$F_{tv}(\alpha) = \pi \left[(r_p)^2 - (r_v)^2 \cos(\alpha) \right] \quad (15)$$

- flow coefficient μ , which depends on pressures ratio across the valve

$$\mu^* = \sqrt{\frac{T_c}{298}} f\left(\frac{p_s}{p_c^*}\right) \quad (16)$$

The pressure and temperature of air outflowing from the turbo-compressor can be found as a function of compressor rotational speed n_{tc} and efficiency η_{ic} in the following form as in 8):

$$\frac{p_c^*}{p_a} = \left\{ \left[\left(\frac{p_{c0}}{p_a} \right)^{\frac{k_a - 1}{k_a}} - 1 \right] \left(\frac{n_{tc}}{n_{tc0}} \right)^2 + 1 \right\}^{\frac{k_a}{k_a - 1}} \quad (17)$$

$$T_c = T_a \left[\frac{1}{\eta_{ic}} \left(\left(\frac{p_c^*}{p_a} \right)^{\frac{k_a - 1}{k_a}} - 1 \right) + 1 \right] \quad (18)$$

3.4 Exhaust gas receiver

The state of exhaust gas in the receiver can be described by the mass balance, the ideal gas law and the first law of thermodynamics however no heat transfer is taken into account. Two differential equations can then be derived determining mass and temperature of gas within the receiver and the pressure is the result of mass, temperature and volume, respectively:

$$\frac{dm_{e,r}}{dt} = G_a + G_f - G_e \quad (19)$$

$$\frac{dT_e}{dt} = \frac{k_e}{m_{e,r} C_{p,e}} (G_a C_{p,a} T_s + G_f H_u \xi_a) - \frac{T_e}{m_{e,r}} \left(G_e k_e + \frac{dm_{e,r}}{dt} \right) \quad (20)$$

$$p_e = \frac{m_{e,r} R_e T_e}{V_{e,r}} \quad (21)$$

The exhaust gas mass flow rate G_e can be estimated similarly to the scavenging air mass flow, considering turbine as a nozzle:

$$G_e = G_a + G_f = a_t \tilde{A}_t \frac{p_e}{\sqrt{R_e T_e}} \left\{ \frac{2 k_e}{k_e - 1} \left[\left(\frac{p_o}{p_e} \right)^{\frac{2}{k_e}} - \left(\frac{p_o}{p_e} \right)^{\frac{k_e + 1}{k_e}} \right] \right\}^{\frac{1}{2}} \quad (22)$$

The accuracy of exhaust gas flow prediction is greatly improved if the correction coefficient a_t for a turbine effective flow area \tilde{A}_t is introduced to the model. It is adequately to describe the correction coefficient as a polynomial function of the turbine pressure ratio p_o/p_e , those coefficients are selected to fit experimental data.

Making use previously obtained mass of gas supplied per cycle $m_{f,c}$, the engine fuel mass flow rate is obtained:

$$G_f = 0.5 z_c m_{f,c} n_e \quad (23)$$

The energy balance Eq.20, applied on the exhaust gas receiver includes the energy of gas leaving a cylinder after combustion. Since the MVEM approach considers only the cycle averaged values, the result of combustion – enthalpy increase of intake air, is considered by the coefficient of fuel chemical energy proportion in the exhaust gas ξ_a , which is the function of the engine brake mean effective pressure (bmep):

$$\xi_a = k_{\xi_1} \ln(\text{bmep}) + k_{\xi_0}, \quad \therefore \text{bmep} = \frac{2\pi}{0.5 z_c V_s} Q_e \quad (24)$$

3.5 Turbo-compressor rotational dynamics

In a turbocharged engine the transient dynamics of turbo-compressor speed is the most dominant dynamics with the notable effect of turbocharger lag. Thus the rotational dynamics of turbo-compressor in terms of speed is modeled using the Newton's second law for rotating system:

$$2\pi I_{tc} \frac{dn_{tc}}{dt} = Q_t(n_{tc}, p_e, \dots, t) - Q_c(n_{tc}, p_c, \dots, t) \quad (25)$$

Making use the previously obtained thermodynamic states of the engine, the torques of compressor and turbine can be obtained by considering the isentropic work required for air compression and isentropic work done by exhaust gas expansion, respectively:

$$Q_c = \frac{C_{p,a} T_a G_{tv}}{2\pi n_{tc} \eta_{ic}} \left(\left(\frac{p_c^*}{p_a} \right)^{\frac{k_a - 1}{k_a}} - 1 \right) \quad (26)$$

$$Q_T = \frac{C_{p,e} T_e G_e \eta_{iT}}{2\pi n_{tc}} \left(1 - \left(\frac{p_o}{p_e} \right)^{\frac{k_e - 1}{k_e}} \right) \quad (27)$$

The expression for compressor torque includes isentropic efficiency η_{ic} , which, for the compressor matched to the engine, can be considered constant. Turbine efficiency η_{iT} is usually expressed as a function of normalized blade speed ratio, as can be found in 9):

$$\eta_{iT} = \eta_{iT_0} - c_T \left(\frac{n_{tc}}{\sqrt{T_e \left(1 - \left(\frac{p_o}{p_e} \right)^{\frac{k_e - 1}{k_e}} \right)}} \frac{\sqrt{T_{e_0} \left(1 - \left(\frac{p_o}{p_e} \right)^{\frac{k_e - 1}{k_e}} \right)}}{n_{tc_0}} \right)^2 \quad (28)$$

The casual signal paths, inputs and internal variables as well as the core governing equations elucidating relationships between the sub-models are shown in Fig.3 and Table 2 respectively. The resulting model has five continuous states and set of strongly nonlinear algebraic equations supplemented with empirical parameters. The important part of model development is the model tuning and validity, both the steady-state and dynamic.

Table 2. Core equations of the MVEM

$p_c = f(n_{tc}^2)$
$G_{tv} = \mu^* \left(\frac{p_s}{p_c^*} \right) F_{tv}(\alpha) \frac{p_c^*}{\sqrt{R_a T_c}} \psi \left(\frac{p_s}{p_c^*} \right)$
$G_a = G_{tr}(n_e, p_s) + G_{sc} \left(\frac{p_e}{p_s} \right)$
$G_f = G_{fv} \left(\frac{p_s}{p_f} \right) d_{inj} n_e$
$G_e = G_a + G_f = A_t \left(\frac{p_o}{p_e} \right) \frac{p_e}{\sqrt{R_e T_e}} \psi \left(\frac{p_o}{p_e} \right)$
$p_e = \frac{m_{e,r} R_e T_e}{V_{e,r}}$
$\frac{dp_s}{dt} = \frac{R_a T_s}{V_{a,r}} (G_{tv} - G_a)$
$\frac{dT_e}{dt} = \frac{k_e}{m_{e,r} C_{p,e}} \left(h_e \{G_a + G_f\} - C_{p,e} T_e G_e - \frac{C_{p,e} T_e}{k_e} \frac{dm_{e,r}}{dt} \right)$
$\frac{dm_{e,r}}{dt} = G_a + G_f - G_e$
$\frac{dn_e}{dt} = \frac{1}{2\pi I_e} (Q_e(d_{inj}, n_e) - Q_l)$
$\frac{dn_{tc}}{dt} = \frac{1}{2\pi I_{tc}} (Q_t(G_e, p_e) - Q_c(G_{tv}, p_c))$

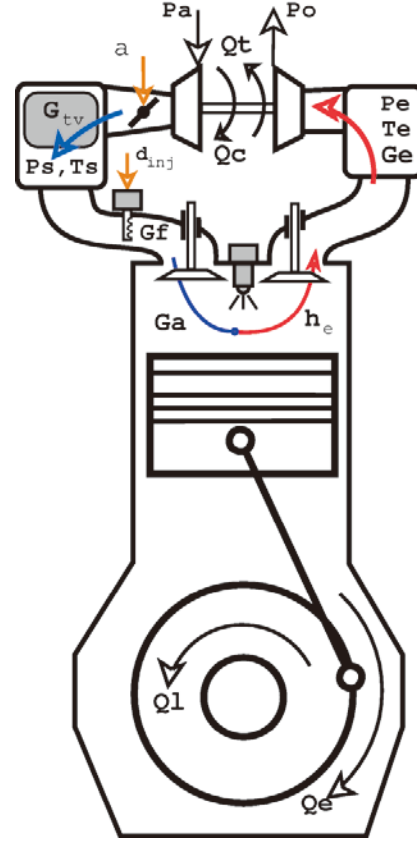


Fig. 3 Variables mutual relationships

4. Model Tuning and Validation

The tuning and validation of the model was done on test data obtained from the test bed engine which was run at two speeds, notably 1500/1800 rpm, and at load ranges from 25% to 100 % of rated power. At first the model parameters were adjusted to satisfy the steady-state performance of the engine, after that the transient test has been performed to check the dynamic performance of the model. From the engine control point of view, the dynamic accuracy of the model is important, however, the steady-state performance is also essential because in the last analysis it determines the reliability and stability of the dynamic model.

The most of the empirical parameters in the engine model can be determined on basis of physical laws and design data of engine. However, there are a number of parameters which have to be matched, in particular a flow coefficient in the throttle valve model and an effective area in the fuel valve model.

4.1 Air throttle and fuel admission valve characteristics

In order to find the proper description of the flow coefficient the engine was run at different throttle valve flap angles providing wide range of pressure ratios across the air throttle valve. Then, by rearranging the Eq.(14) the values of flow coefficients were obtained. In the case of air throttle valve the dependence of flow coefficient on a pressure ratio is strongly nonlinear as can be seen in Fig.4a, especially in the region where the pressure ratio close to unity. In order to catch this nonlinearity, the following implicit function is proposed:

$$\frac{p_s}{p_c} = 1 - k_1 \exp\left(-\frac{\mu}{k_2}\right) - k_3 \exp\left(-\frac{\mu}{k_4}\right) \quad (29)$$

The validity of the proposed model for the throttle valve and flow coefficient was confirmed by comparing measured air mass flow with that calculated by Eqs. (14, 15, 16 and 29). The results are reported in Fig.4b and it is clear that the predictions of the model are fairly well.

In the case of the fuel admission valve the geometrical flow area doesn't change in operation, moreover it is unknown, so what is sought here is the effective flow area F_{fv} which is the product of a flow coefficient and the geometrical flow area. Here it should be noted that the gas pressure in the fuel line is changed proportionally to the air manifold pressure, this implies that the pressure ratio is kept far from unity (strongly nonlinear region) in order to ensure stable and sufficient gas flow into intake port. Following the same procedure as in the case of air throttle valve, the values of effective flow area are obtained and depicted in Fig.5b, and the fuel pressure control curve is shown in Fig.5a. It is clearly evident that the both characteristics can be approximated by simple linear functions of the following form:

$$F_{fv} = f_0 + f_1 \frac{p_f}{p_s} \tag{30}$$

$$p_f = c_0 + c_1 p_s \tag{31}$$

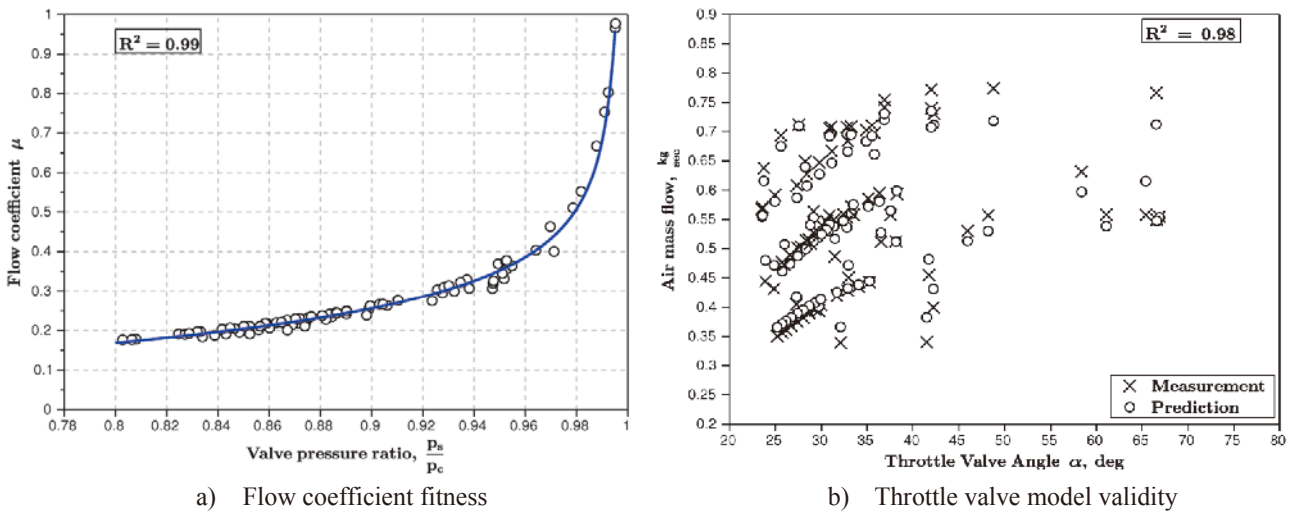


Fig. 4 Air throttle valve characteristics

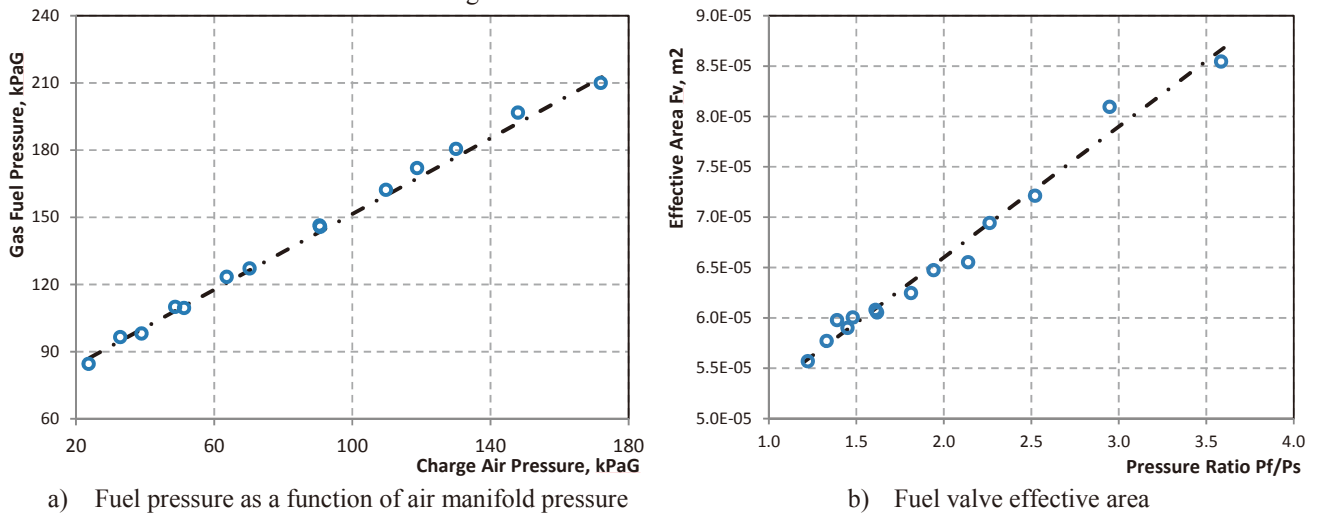


Fig. 5 Fuel admission valve characteristics

The proposed model of fuel admission valve provides maximum error $\pm 5\%$ of fuel flow estimation; the similar results were also obtained in [10]. Last but not least remark regarding the model is that the fuel gas flow expressed by Eq.(7) can now be considered as a function of air manifold pressure only.

4.2 Model stationary similarity

After tuning the empirical parameters and confirming similarity of the sub-models, the total engine model was evaluated at steady-state and the predicted values were compared to that of actual engine values. The Fig.6 summarizes the comparison of key engine performance parameters such as the charge air/exhaust gas pressures, exhaust gas temperature across the turbine, fuel mass and air mass flows. As can be seen the developed model provides fairly well predictions.

As soon as the steady-state similarity is confirmed, only a limited number of parameters, affecting the dynamic response have to be tuned. These are engine and turbo-compressor moments of inertia, volumes of air and exhaust gas receivers, governor coefficients.

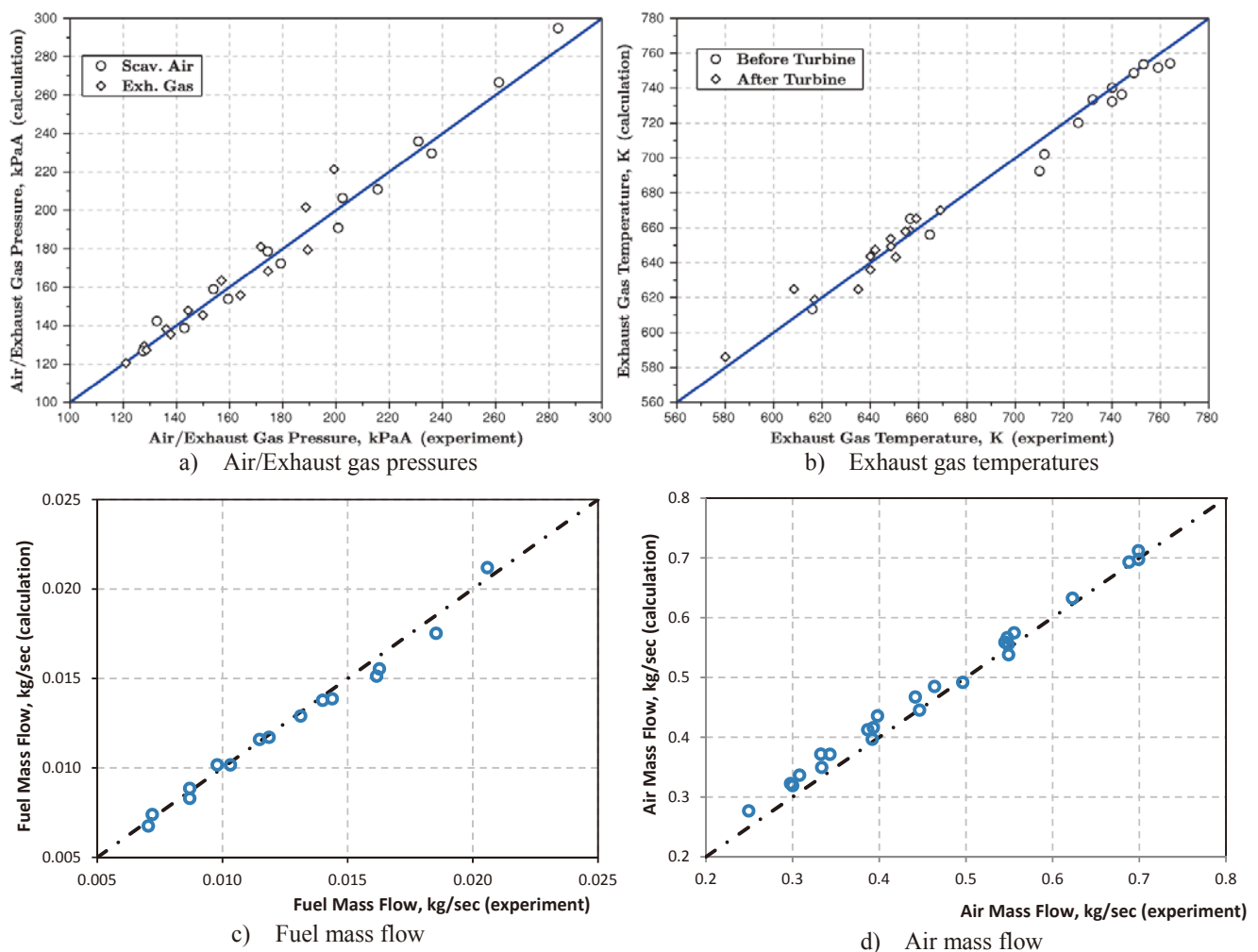


Fig. 6 Comparison of actual engine parameters with model predictions for operation at 1500/1800 rpm speeds

4.3 Model dynamics similarity

Besides of the engine inherent dynamic, the parameters of control loops have a significant influence on the total system dynamic. In the engine under consideration, the speed is stabilized by a PID feedback governor which adjusts fuel gas admission time d_{inj} . The air manifold pressure is controlled by a PID feed-forward governor which adjusts the angular position of throttle valve flap depending on the alternator power. It is difficult to determine the governor coefficients, as

adjusted on the engine, with accuracy. Thus the parameters of the control loops were identified from the measured transient responses.

Fig.7 shows the engine parameters transient transition, measured and predicted, as a result of alternator power step increase. At the initial state the engine was run at 1800 rpm delivering 50% of rated power, then the alternator power was set to 75% of rated (step increase) and the dynamics of the engine parameters were measured.

From the Fig.7a some discrepancy can be observed between measured and simulated control inputs. This is, perhaps, the result of rough identification control loops parameters. Further it can be concluded, that the simulated response of air manifold pressure lacks somewhat dynamic overshoot. This difference between reality and model could be attributed to unaccounted dynamics of air mass acceleration or uncertainty of turbo-compressor mass moment of inertia and manifolds volumes. At the same time prediction of engine speed and turbo-compressor speed transients stay in good agreement with the experiment, these imply that a reasonable prediction of the engine dynamics has been realized.

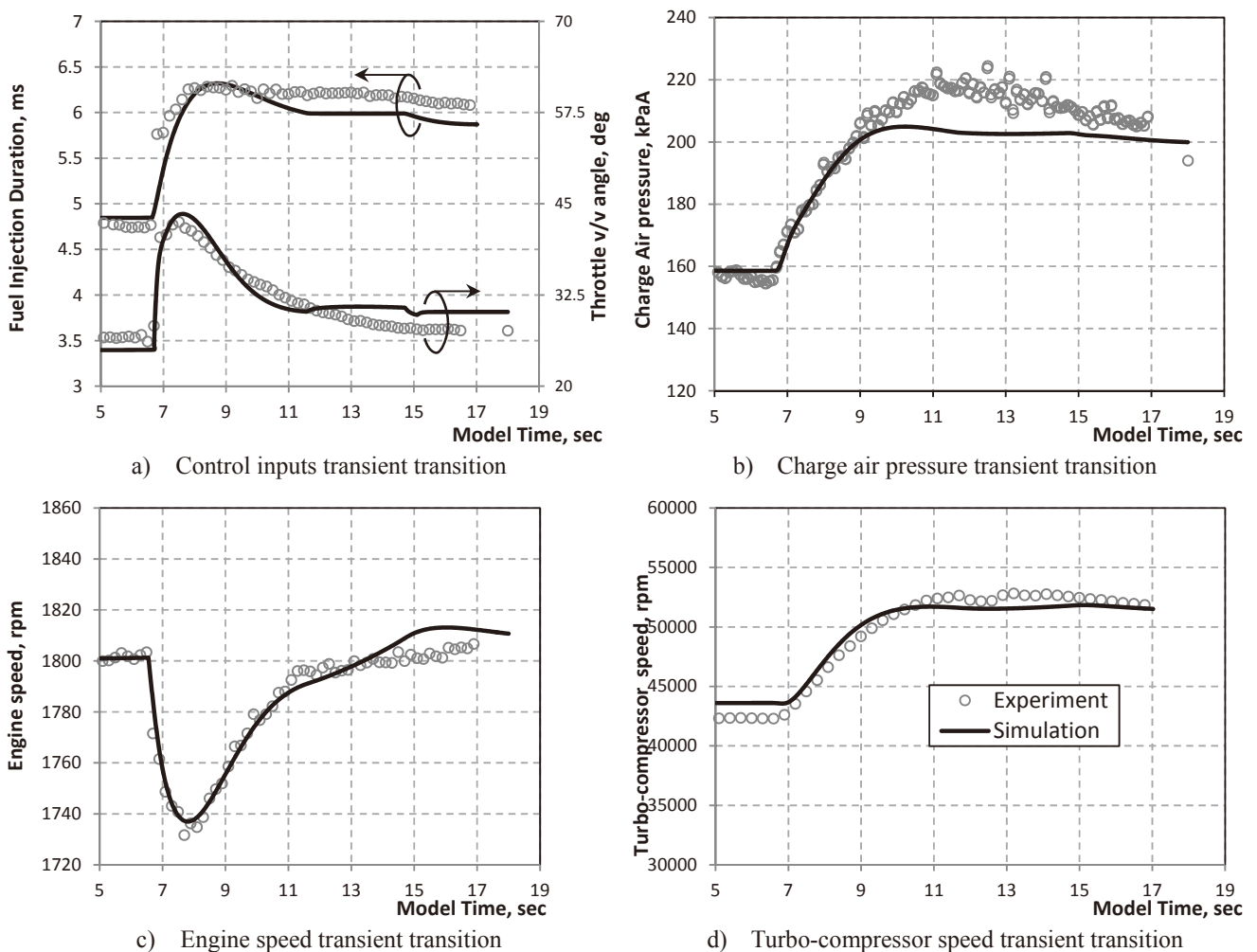


Fig. 7 Engine responses to the alternator power step increase

5. The model utilization

The developed nonlinear model of the lean-burn gas engine can be used for the simulation of the dynamic behavior of different drive systems. However, the model is of special interest for purpose of control system design – so called “design by simulation”. Following the controller design, the strategies found are tested using model simulation – Software in the Loop (SIL) approach. In this way, the global stability of the control system can be confirmed over a wide operating range without the need for extensive actual engine experiments.

5.1 Control systems study

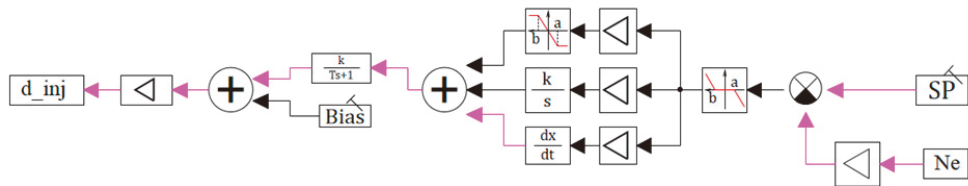
In this chapter the performance difference of three different types of governors is considered. The structural diagrams of governors are depicted in Fig.8. In Fig.8a and 8b conventional speed governors are presented. These types of governors found wide spread in maritime application owing to their simplicity and performance. The input is the engine speed deviation and the output is a correction of fuel mass supplied per cycle. The governor in Fig.8a has a classical PID structure with three tuning parameters, notably proportional gain, integral gain and differential gain. The governor on Fig.8b is the proportional governor with stabilizing PI feedback. This kind of structure is typical for Woodward PG or PGA type governors. The tuning parameters are proportional gain, internal feedback gain and time constant.

The gains adjustment for above mentioned governors can be done by various techniques satisfying various performance criteria. The details can be found in [11], [12] and are out of scope in this paper. However the performance criteria for the Diesel engine and the lean-burn gas engine are somewhat different. This is because gas engine combustion process is sensitive to air-to-fuel ratio; in turn the air-to-fuel ratio variation in transient process is a common phenomenon due to the turbo-compressor lag. The last cause, in fact, determines the application of additional control loops, like the air throttle valve, to diminish the effect of turbo-compressor lag.

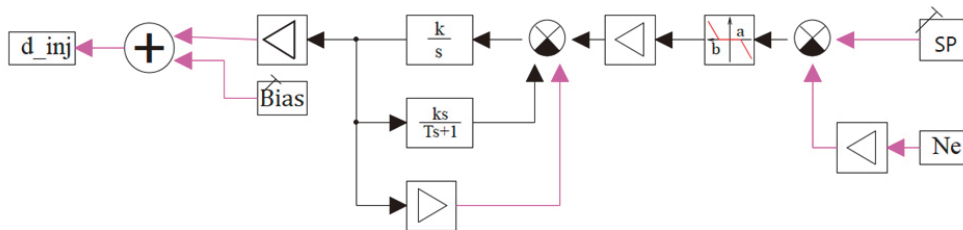
The air-to-fuel ratio λ is a dimensionless variable defined as the ratio between the actual and the stoichiometric air-to-fuel ratio L_o , namely

$$\lambda = \frac{G_a}{G_f L_o} \tag{32}$$

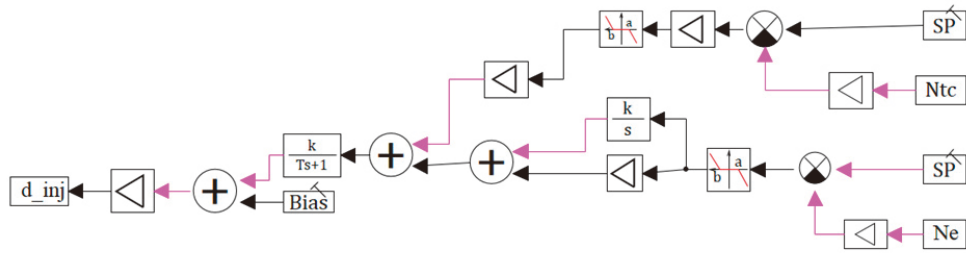
The air mass flow G_a is primarily determined by the air manifold pressure which in turn is a function of throttle valve flap position and turbo-compressor speed. The fuel mass flow G_f is the function of the fuel admission time d_{inj} . When the engine load rapidly increases, the speed governor responds very fast, immediately increasing the fuel mass flow. However the turbo-compressor speed buildup delays due to inertia and the air mass flow does not follow fuel mass flow which eventually leads to a temporal operation on a rich gas-air mixture and may provoke knocking. In this respect introduction of an additional input, notably turbo-compressor speed, to control structure may improve transient response playing role of a fuel limiter. This concept is realized as a MIMO (multi input – multi output) speed governor, structural diagram of which is depicted in Fig.8c. The standard PI engine speed governor is supplemented with the Proportional turbo-compressor speed governor, and their combined action generates the control signal.



a) Classical PID governor



b) Woodward-type P+PI governor



c) MIMO type governor (two input one output)

Fig.8 The considered speed governors

In the simulation, the engine transient performance to 25% load step increase, with all type controllers was investigated. The results are reported in Fig.9. The parameters of governors were modified in order to reduce engine speed drop and also improve speed recovery time, and the same time constraint was imposed on air-to-fuel ratio drop. From the figure it is clearly seen that introduction of additional input signal favorably affects the transient performance of the engine, notably both the engine speed drop and recovery time has been reduced with no penalties in terms of air-to-fuel ratio. At the same time it should be noted that the governor’s gains adjustment is a tough task since the number of parameters, criteria and constraints are large and both control loops appeared to have mutual ambiguous influence on transient performance. In fact ‘design by simulation’ approach is very time consuming. Thus it is necessary to consider the modern, rigorous theoretical methods of control systems design. However, the methods of modern control theory require the model to be linearized and represented in a state space form. Despite the fact that the developed engine model is strongly nonlinear, the constituent variables hold explicit functional relationships with the dynamic variables. This creates prerequisites for deriving linearized model analytically as discussed in the next paragraph.

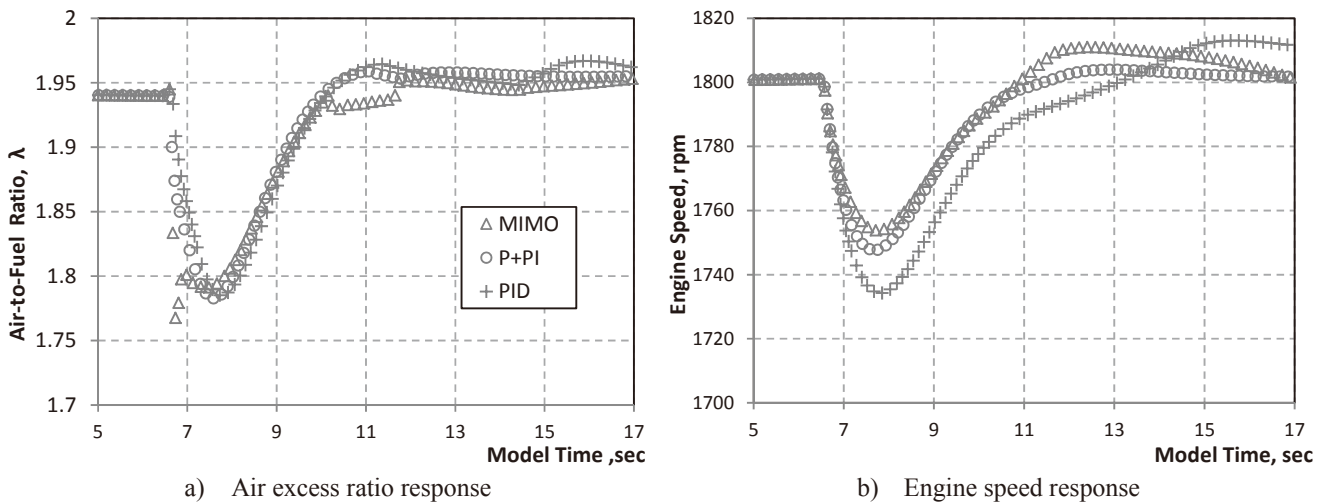


Fig. 9 Control system responses compare

5.2 Linearized state space engine model

In order to find the requisite small signal response, the nonlinear engine model should be linearized in the vicinity of an arbitrary operating point, and then the vector matrix of the linearized state space system can be described as follows:

$$\begin{aligned} \delta \dot{x} &= A\delta x + B\delta u \\ \delta y &= C\delta x + D\delta u \end{aligned} \tag{33}$$

Where $\delta \mathbf{x}$ denotes vector of incremental system states, $\delta \mathbf{y}$ denotes the vector of incremental system outputs and $\delta \mathbf{u}$ denotes the vector of incremental system inputs. \mathbf{A} and \mathbf{B} are the Jacobian matrixes evaluated on functions describing the system at the desired operating point.

In order to use the linearized model it is, of course, necessary to find the values of the matrix elements at the desired linearization point and this can be done numerically. However the analytical approximation, true within a certain range, can also be obtained employing the method of small increments¹³⁾. The advantage over a numerical solution is that it bound up with an initial equation from which some insight can be gained.

In compliance with the method of small increments, the composite nonlinear function is transformed to a linear combination of constituent variables as follows:

- Arbitrary nonlinear function:

$$F = c f_1(x_1) \dots f_n(x_n) \quad (34.1)$$

- is decomposed by applying logarithm:

$$\ln(F) = \ln(c) + \ln(f_1(x_1)) + \dots + \ln(f_n(x_n)) \quad (34.2)$$

- then, partial differentiation is performed:

$$\frac{dF}{F} = \frac{\partial f_1(x_1)}{\partial x_1} \frac{dx_1}{f_1(x_1)} + \dots + \frac{\partial f_n(x_n)}{\partial x_n} \frac{dx_n}{f_n(x_n)} \quad (34.3)$$

- introducing coefficient of influence and substituting small increment for differential, the resulting linearized function is obtained:

$$k_i = \frac{\partial f_i(x_i)}{\partial x_i} \frac{x_i}{f_i(x_i)}, \quad \frac{dF}{F} \approx \frac{\Delta F}{F} \approx \delta F \quad (34.4)$$

$$\delta F \approx k_1 \delta x_1 + \dots + k_n \delta x_n$$

For the sake of simplicity and illustration the application of the introduced method, the nonlinear equation of air mass flow through the throttle valve will be linearized hereinafter.

At first let's consider the standard linearization technic such as the Taylor series expansion keeping first-order term only. The air mass flow $G_{tv} = f(p_c, p_s, \alpha)$ is the nonlinear function of three variables, and its small perturbation $\Delta G_{tv} = G_{tv}(p_c, p_s, \alpha) - G_{tv}(p_{c_0}, p_{s_0}, \alpha_0)$ can be obtained as below:

$$\Delta G_{tv} \approx \frac{\partial G_{tv}}{\partial p_c} \Delta p_c + \frac{\partial G_{tv}}{\partial p_s} \Delta p_s + \frac{\partial G_{tv}}{\partial \alpha} \Delta \alpha \quad (35)$$

Then, introducing relative values of partial derivatives and variables, one may obtain:

$$\begin{aligned} \frac{\partial G_{tv}}{G_{tv_0}} \frac{p_{c_0}}{\partial p_c} \frac{\Delta p_c}{p_{c_0}} &= \frac{\delta G_{tv}}{\delta p_c} \delta p_c \\ \delta G_{tv} &\approx \frac{\delta G_{tv}}{\delta p_c} \delta p_c + \frac{\delta G_{tv}}{\delta p_s} \delta p_s + \frac{\delta G_{tv}}{\delta \alpha} \delta \alpha \end{aligned} \quad (36)$$

At the same time the throttle valve air mass flow is expressed by the explicit function as Eq.(14) and following the method of small increment, linearization yields:

$$\begin{aligned}
 G_{tv} &= \mu^* F_{tv}(\alpha) \frac{p_c^*}{\sqrt{R_a T_c}} \Psi \left(\frac{p_s}{p_c^*} \right) \\
 &\quad \downarrow \\
 \ln(G_{tv}) &= \ln(\mu) + \ln(F_{tv}) + \ln(p_c^*) - 0.5 \ln(R_a T_c) + \ln(\Psi) \\
 &\quad \downarrow \\
 \frac{\partial G_{tv}}{G_{tv_0}} &\approx \frac{\partial \mu}{\mu_0} + \frac{\partial F_{tv}}{F_{tv_0}} + \frac{\partial p_c}{p_{c_0}} + \frac{\partial \Psi}{\Psi_0} \\
 &\quad \downarrow \\
 \delta G_{tv} &\approx \delta \mu + \delta F_{tv} + \delta p_c + \delta \Psi
 \end{aligned} \tag{37}$$

Further, some constituent variables are not yet independent, for instance valve flap projection area F_{tv} which also holds functional relationship with flap angle α , thus applying again the method of small increments yields:

$$\begin{aligned}
 F_{tv}(\alpha) &= \pi \left[(r_p)^2 - (r_v)^2 \cos(\alpha) \right] \\
 &\quad \downarrow \\
 \delta F_{tv} &\approx \underbrace{\left[\left(\frac{\pi (r_p)^2 - F_{tv_0}}{F_{tv_0}} \right) \alpha_0 \tan(\alpha_0) \right]}_{K_{F_{tv}}} \delta \alpha
 \end{aligned} \tag{38}$$

Finally, the linearized equation of the air mass flow through the throttle valve transforms to:

$$\delta G_{tv} \approx (1 - K_\psi - K_{p_c} K_\mu) \delta p_c + (K_{p_c} K_\mu + K_\psi) \delta p_s + K_{F_{tv}} \delta \alpha \tag{39}$$

Now, if the terms of Eq.(39) are compared with the corresponding terms of Eq.(36), one may find similarity in that the relative values of partial derivatives in the Taylor series expansion correspond to the influence coefficients of the method of small increments. But in the last case the coefficients are bound up with the original nonlinear equation and their values can be easily evaluated at arbitrary operating point of the engine.

As the result of linearization, the engine model can be represented in state space form as Eq.(33), where:

$$\begin{aligned}
 \delta \mathbf{x} &= [n_e, n_{tc}, p_s, m_{e,r}, T_e]^T, \quad \delta \mathbf{y} = \delta \mathbf{x}, \quad \delta \mathbf{u} = [\delta d_{inj}, \delta \alpha, \delta Q_l]^T \\
 \mathbf{A} &= \begin{bmatrix} a_{1,1} & 0 & a_{1,3} & a_{1,4} & a_{1,5} \\ 0 & a_{2,2} & a_{2,3} & a_{2,4} & a_{2,5} \\ a_{3,1} & a_{3,2} & a_{3,3} & a_{3,4} & a_{3,5} \\ a_{4,1} & 0 & a_{4,3} & a_{4,4} & a_{4,5} \\ a_{5,1} & 0 & a_{5,3} & a_{5,4} & a_{5,5} \end{bmatrix} \\
 \mathbf{B} &= \begin{bmatrix} b_{1,1} & 0 & b_{1,3} \\ 0 & b_{2,2} & 0 \\ 0 & b_{3,2} & 0 \\ b_{4,1} & 0 & 0 \\ b_{5,1} & 0 & 0 \end{bmatrix}
 \end{aligned} \tag{40}$$

The important question remained – what is the trust region of the linearized model? This question can be answered if the responses of original nonlinear model be compared with that of linearized model. Fig.10 shows the comparison of key variable responses to 10% load input. Clearly, the linearized analytical model conforms the original nonlinear model of the engine and this implies that it can be used for control system investigation and development.

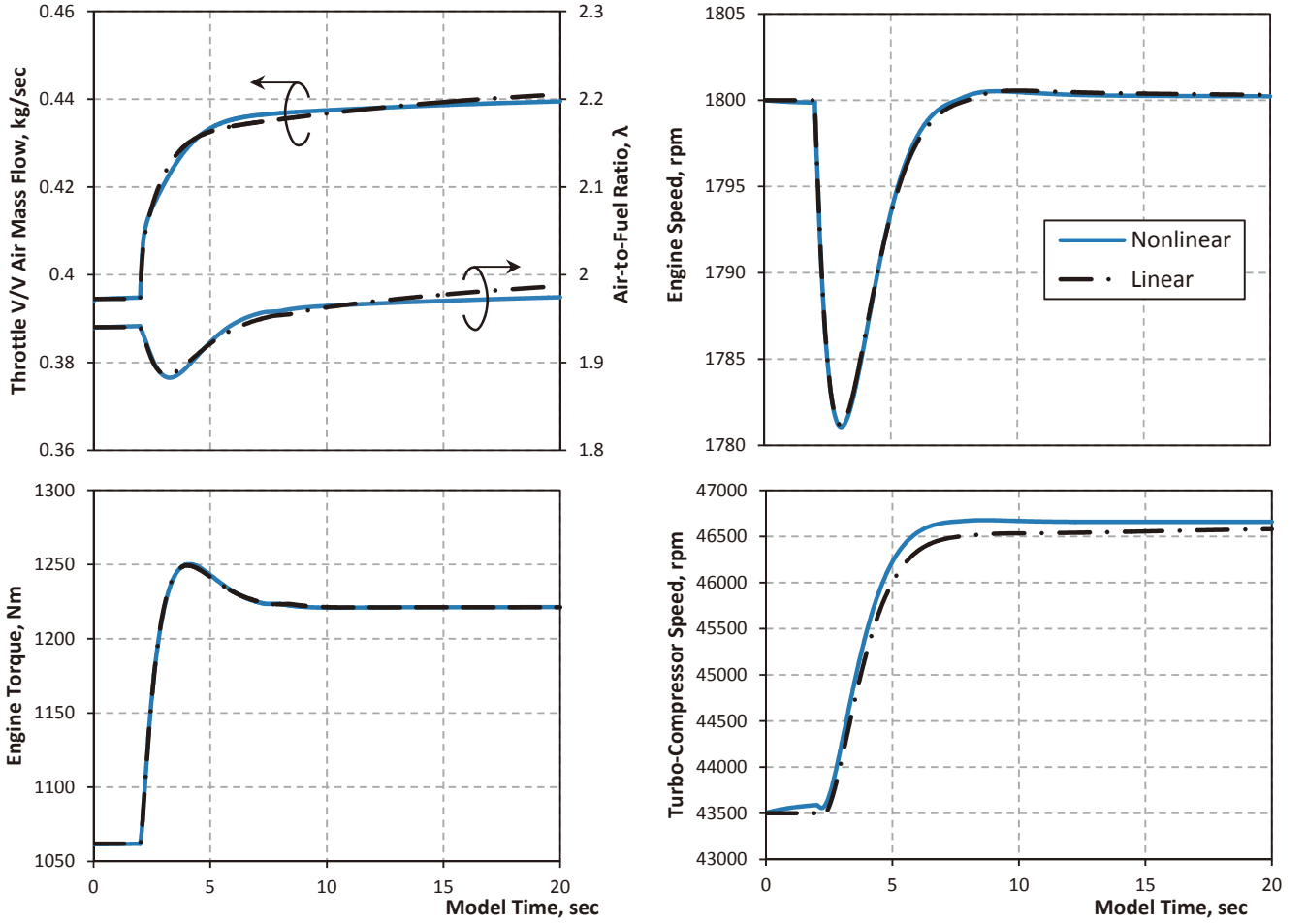


Fig. 10 Linearized model comparison

5.3 Analysis of system robustness

Needless to say that the simulation model is just an approximation of the real physical system, and, in any case, the parameters involved in such an approximation are often subject to variation and uncertainty. It is therefore important, in the analysis stage, to assess the sensitivity of the system stability and performance to parameter variations. This can be done by the analysis of a system response function behavior to variation of specific model parameter in frequency domain. The system response function is defined as a ratio of desired output to control input, and from the state space description of the system it can be readily obtained, namely

$$W(s) = \frac{\delta y}{\delta u} = \mathbf{C}(s\mathbf{I} - \mathbf{A})^{-1}\mathbf{B} + \mathbf{D} \quad (41)$$

With respect to the lean-burn gas engine the desired system output to be investigated is, beyond dispute, air-to-fuel ratio. However, it does not readily available as the system state and has to be obtained by manipulating the available states. This easily can be done considering the Eqs.(32, 23, 13) and following the method of small increments, the transformation yields:

$$\delta\lambda = (K_{G_{a.n_e}} - 1)\delta n_e + 0 \delta n_{tc} + (K_{G_{a.p_s}} - K_{f.v.p_s})\delta p_s + K_{G_{a.p_e}}(\delta T_e + \delta m_{e,r}) - \delta d_{inj} \quad (42)$$

Thus the obtained relation of air-to-fuel ratio with state variables is reflected in matrices \mathbf{C} and \mathbf{D} , namely

$$C = \begin{bmatrix} \lambda_{1,1} & 0 & \lambda_{1,3} & \lambda_{1,4} & \lambda_{1,5} \\ 0 & 0 & 0 & 0 & 0 \\ 0 & 0 & 0 & 0 & 0 \\ 0 & 0 & 0 & 0 & 0 \\ 0 & 0 & 0 & 0 & 0 \end{bmatrix}, \quad D = \begin{bmatrix} -1 & 0 & 0 \\ 0 & 0 & 0 \\ 0 & 0 & 0 \\ 0 & 0 & 0 \\ 0 & 0 & 0 \end{bmatrix} \quad (43)$$

The response function behavior in frequency domain is conveniently represented by the Bode plot, substituting complex frequency $i\omega$ for Laplace operator s in Eq.(41) and expressing the magnitude in decibels:

$$H = 20 \log_{10}|W(i\omega)|, \quad \text{db} \quad (44)$$

As was observed from engine experiments, one of the important sub-system influencing engine steady-state and transient performances is the air throttle valve and its flow coefficient represents the major uncertainty of the air mass flow calculation thus, directly affecting air-to-fuel ratio estimation. The model robustness is investigated varying the throttle valve flow coefficient by $\pm 25\%$ with respect to the base characteristics as shown in Fig.11a. The Bode plots are reported in Fig.11b. The upper plot shows the air-to-fuel ratio response to throttle valve flap angle $H(\lambda/\alpha)$, and lower plot shows the response to fuel admission time $H(\lambda/d_{inj})$.

The performed investigation confirmed the importance of the throttle valve characteristics on the engine transient behavior. Although the stability is not violated, the reduced flow coefficient (Set 1) introduces oscillations to the response characteristic and at the same time improves the recovery time of air-to-fuel ratio in response to the fuel admission time.

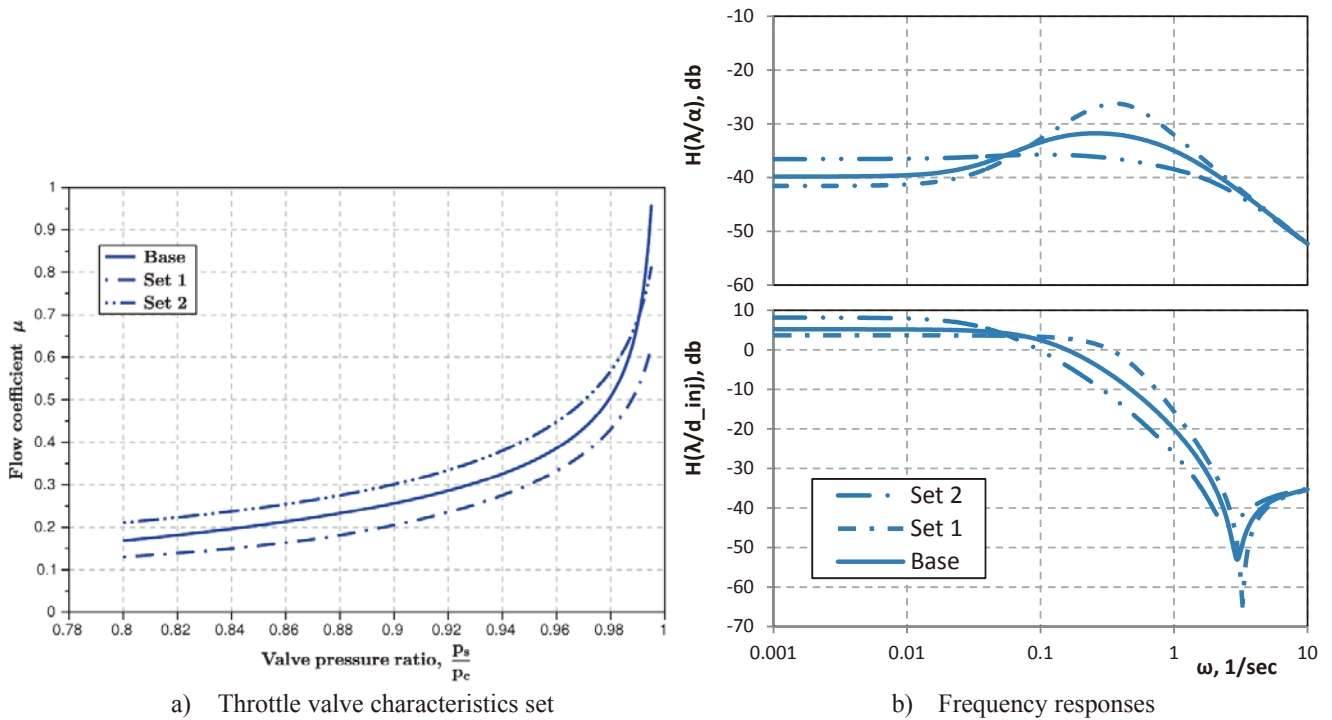


Fig.11 Control system sensitivity

6. Conclusions

The developed model, presented in this paper, has proven to be suitable for the simulation of the dynamic behavior of the lean-burn gas engine drive system. The model is fully parametrized and its structural design can be easily modified for another engine type, and also modifications necessary to introduce additional components, for instance EGR system or Exhaust Bypass Valve, are of small complexity.

Furthermore the developed model is especially suitable for control system design by simulation, which was utilized to compare three different governor models. The performed investigation showed that introduction of additional input signal, notably turbo-compressor speed, favorably affects the transient response. At the same it was noted that “design by simulation” methodology lacks rigorous theoretical method of controller pre-design and sensitivity/uncertainty study.

In order to improve the ‘design by simulation’ methodology, the companion linearized state-space model was derived analytically utilizing the method of small increments. The parameters of the derived state space system bound up with the original nonlinear model, thus extending the control system design tool: following the transition of engine model to the desired operating point, the coefficients of state space system matrices are obtained, and then the control system design and sensitivity study are performed, and finally the strategies found are tested on nonlinear engine model. This process can conveniently be repeated at any operating point of the engine providing that the global stability and performance of control system are ensured.

Last but not least, the developed state-space model can be used for developing physically based algorithms of the control loop thus enhancing accuracy of the lean-burn gas engine control. This is the subject for further study.

References

- 1) Rothe, M, Heidenreich, T., et al., 2006, Knock Behavior of SI-Engines: Thermodynamic Analysis of Knock Onset Locations and Knock Intensities, SAE Technical Paper 2006-01-0225
- 2) Hendricks, E., Sorenson C. S., 1991, SI Engine Controls and Mean Value Engine Modeling, SAE Technical Paper 910258
- 3) Klein Woud, J., Boot, Ph., Riet, B.J., 1993, A Diesel Engine Model For the Dynamic Simulation of Propulsion System, Transportation Research Board
- 4) Hansen, J.M., Zander, C.G., et al., 2013, Modeling for Control of Exhaust Gas Recirculation on Large Diesel Engines, In Proc.: 9th IFAC Conference on Control Applications in Marine Systems, CAMS 2013
- 5) Bondarenko O., Kashiwagi, M., 2010, Dynamic Behavior of Ship Propulsion Plant in Actual Seas, *Journal of the Japan Institute of Marine Engineers*, Vol. 45, pp76-80
- 6) Bondarenko O., Fukuda T., et al., 2015 Novel Concept of Inverter-less Electric Drive for Ship Propulsion System. *Journal of the Japan Institute of Marine Engineers*, Vol. 50, pp76-80
- 7) Theotokos G.P., 2009, A Comparative Study on Mean Value Engine Modeling of Two-Stroke Marine Diesel Engine., In Proc.: The 2nd International Conference on Maritime and Naval Science and Engineering
- 8) Bondarenko O., Fukuda T., et al., 2013, Development of Diesel Engine Simulator for Use with Self-Propulsion Model. *Journal of the Japan Institute of Marine Engineers*, Vol. 48, pp 98-105
- 9) Erikson, L., 2007, Modeling and Control of Turbocharged SI and DI Engines, *Oil & Gas Science and Technology – Rev. IFP*, Vol 62, No.4, pp. 523-538
- 10) Vrublevskiy, A., Dzyubenko, A., et al., 2014, Determination of Flow Rate in Gas Engine with Electronic Control of Fuel Delivery System (in Russian), *Internal Combustion Engines*, Issue 2, pp 33 – 36
- 11) Kirk, D.E., 2012, *Optimal Control Theory: An Introduction*, Courier Dover Publications: Mineola, NY, USA
- 12) Ogata, K., 2010, *Modern Control Engineering*, Pearson Education: New York, USA
- 13) Cherkez, A., 1975, Engineering design of the turbocharged engines employing method of small increments (in Russian), Mashinostroenie, Moscow.